

**Published as:**

AKHTAR, M. U. & FOCKE, W. W. 2015. Trapping citronellal in a microporous polyethylene matrix. *Thermochimica Acta*, 613, 61-65.

## **Trapping citronellal in a microporous polyethylene matrix**

Mohamed U Akhtar and Walter W Focke\*

UP Centre for Sustainable Malaria Control and Institute of Applied Materials, Department of Chemical Engineering, University of Pretoria, Private Bag X20, Hatfield 0028, Pretoria, South Africa

**Abstract**

The Flory-Huggins theory was used to model the phase behaviour of linear low density polyethylene-citronellal binary mixtures. The model parameters were obtained from fitting the bimodal phase envelope using data points from cloud point determinations. This allowed the prediction of the melting point depression curve as well as the location of the spinodal region. A microporous polyethylene matrix was obtained by quenching homogeneous liquid mixtures at temperatures well below the spinodal phase boundary. This strategy makes it possible to trap, and effectively solidify, large amounts of citronellal in a polyethylene (LLDPE) matrix. This has potential implications for the development of long-lasting insect repellent bracelets and anklets.

**Keywords:** Citronellal; polyethylene; phase separation; microporous

\*Corresponding author: Phone: (+27) 12 420 3728; Fax: (+27) 12 420 2516; e-mail:

[walter.focke@up.ac.za](mailto:walter.focke@up.ac.za)

## 1. Introduction

Thermally induced phase separation (TIPS) [1, 2] can yield microporous polymer structures that are of practical interest [3]. Many different shapes and forms, e.g. films, sheets, blocks, and more intricate shapes can be made from thermoplastic polymers such as polyolefins. The process yields relatively homogeneous, three-dimensional cellular structures with the cells interconnected by small pores [4]. Microporous polyolefin structures have been studied extensively for numerous reasons including the fact that they represent a low cost option [5-7].

The TIPS process [1] involves heating a polymer-diluent mixture to a sufficiently high temperature where it forms a single homogenous phase. The diluent is usually a low molecular weight, high boiling point solvent in which the polymer is effectively insoluble at room temperature. When the homogenous solution is cooled sufficiently fast to low enough temperatures, the liquid-liquid phase separation occurs via spinodal decomposition. This type of phase separation results in the formation of co-continuous phases. Upon further cooling, the matrix phase solidifies, e.g. by crystallization. The end result is a solid microporous polymer structure that retains the liquid diluent [1].

In most applications the diluent is extracted leaving behind the open-cell microporous polymer skeleton. However, the present objective was to investigate the possibility of trapping larger amounts of an insect repellent in the polymer matrix for controlled release applications. It is also possible to dissolve repellent in suitable polymer matrices. In the loaded state such polymers are swollen by the dissolved insect repellent. So, over time, they will shrink in tandem with the release of the active. Such dimensional instability is undesirable in products such as insect repellent bracelets and anklets. In this study, the phase behaviour of mixtures of citronellal and linear low density polyethylene (LLDPE) was studied using thermal analysis techniques and modelled with Flory-Huggins theory. The

objective was to see whether the TIPS process can be used to, in effect, convert citronellal liquid into a solid form by trapping it a microporous polyethylene matrix.

## 2. Experimental

### 2.1. Materials

Linear low density polyethylene (LLDPE) powder (Grade HR 411: MFI 3.5 @190 °C, 2.16 kg); density 0.939 g cm<sup>-3</sup>; particle size: 90% < 600 μm) was supplied by Sasol Polymers. According to the manufacturer, the number average molar mass (Mn) of this material was 50447 Daltons while the polydispersity index was 3.37. Citronellal (3,7-dimethyloct-6-en-1-al), ethanol (97%) and ethylene glycol were obtained from Merck Chemicals and used as received without further purification. According to the manufacturer the purity of the citronellal was > 93.5%.

### 2.2. Methods

**Microporous sample preparation.** Mixtures of LLDPE and citronellal were prepared at mass ratio of 40:60. The mixtures were wrapped in aluminium foil in a way designed to prevent the repellent from escaping upon heating. The samples were placed in an oven at 150 °C for 1.5 h to allow for homogenization. The samples were then quench-cooled by rapid immersion in mixtures of ethanol with ethylene glycol slurried with crushed dry ice. Different ethanol-ethylene glycol compositions were selected in order to obtain quenching temperatures of -18 °C, -14 °C and 5 °C.[8] An additional sample was quenched in liquid nitrogen (temperature ca. -170 °C).

## 2.3. Characterization

### 2.3.1. Differential scanning calorimetry (DSC)

All the samples were sealed in 50  $\mu\text{L}$  aluminium pans. Differential scanning calorimetry (DSC) was performed on a Perkin Elmer DSC 4000 instrument in a nitrogen atmosphere. The experimental protocol was as follows: Initial temperature of 30  $^{\circ}\text{C}$ ; heated to 145  $^{\circ}\text{C}$  at a scan rate of 10  $^{\circ}\text{C min}^{-1}$ ; held at 145  $^{\circ}\text{C}$  for 5 min and cooled to 30  $^{\circ}\text{C}$  at a cooling rate of 10  $^{\circ}\text{C min}^{-1}$ , and then held at 30  $^{\circ}\text{C}$  for 5 min. This heating cycle was repeated at least twice at a faster heating rate of 40  $^{\circ}\text{C min}^{-1}$  before data collection commenced.

### 2.3.2. Hot stage optical microscopy (OM)

A Leica DM2500M optical microscope fitted with a Leica DFC420 video camera and Linkam CSS 450 hot stage was used to determine the cloud point temperature ( $T_{\text{cloud}}$ ). This was taken as the highest solution temperature where the onset of turbidity was observed. Mixtures of LLDPE and citronellal were subjected to the same temperature scanning protocol used for the DSC data collection. The only difference was that the temperature cycle was repeated at least twice at a scan rate of 30  $^{\circ}\text{C min}^{-1}$  before data was recorded.

### 2.3.3. Field Emission Scanning Electron Microscopy (FESEM)

Samples prepared for determining quenching temperatures were repeatedly washed with acetone to remove the citronellal from the polymer matrix. They were then allowed to dry at ambient conditions. The dried samples cooled in liquid nitrogen and fractured. A graphite coating was deposited before they were observed with a Zeiss Ultra 55 Field Emission Scanning Electron Microscopy at an acceleration voltage of 2 kV.

### 3. Results and discussion

#### 3.1. Differential scanning calorimetry (DSC)

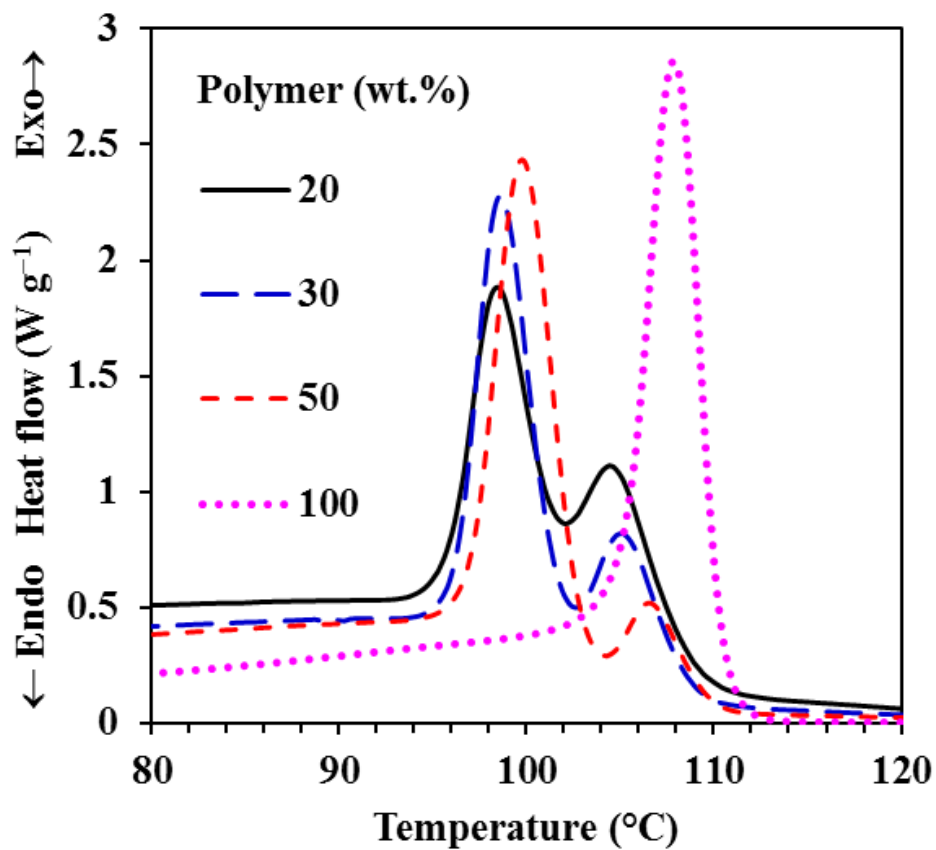


**Figure 1.** Representative DSC crystallization curves for LLDPE-citronellal mixtures obtained at a scan rate of  $10\text{ }^{\circ}\text{C min}^{-1}$  clearly showing the de-mixing exotherms. The heat flow has been normalized with respect to the amount of polymer present.

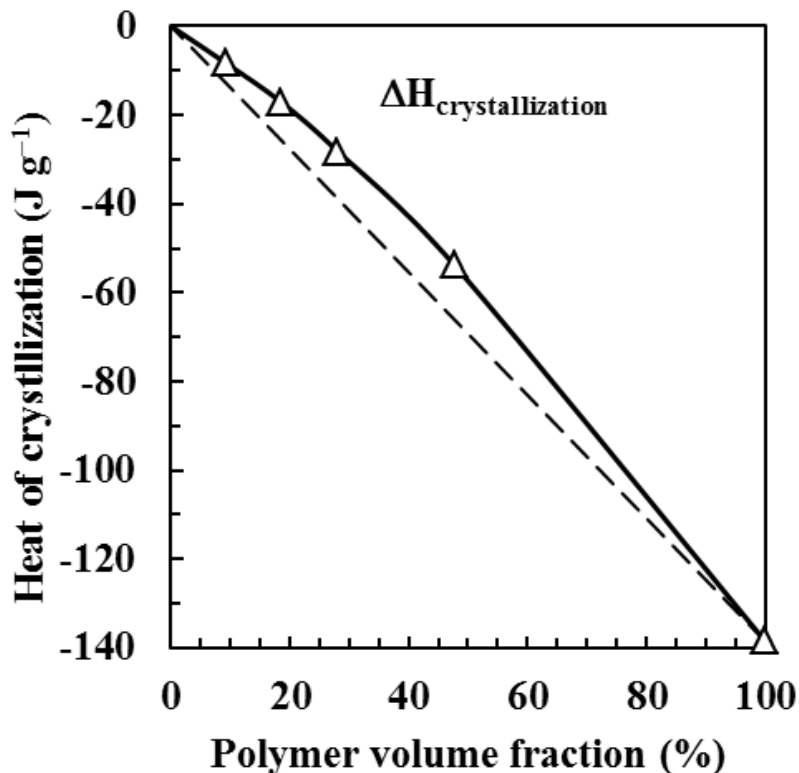


**Figure 2.** Estimated DSC crystallization enthalpies for LLDPE citronellal mixtures measured at a scan rate of  $10\text{ }^{\circ}\text{C min}^{-1}$ . The dotted line indicates the predictions of the linear blending rule.

Figure 1 shows representative DSC cooling curves for LLDPE-citronellal mixtures. The curves in Figure 1 suggest that liquid-liquid phase separation occurred before polymer crystallization commenced. In addition, the position of the crystallization peak shifted to lower temperatures as the citronellal content increased. The experimental heat of crystallization at different mixing ratios is shown in Figure 2. If the presence of the citronellal did not affect the crystallization of the polyethylene, the heat of crystallization would scale linearly with the mass fraction polymer present. This expectation is plotted as the dotted line in Figure 2. The deviation, of the experimental values from these predictions, indicates that not all of the polyethylene crystallized. At 50 wt.% polymer the measured heat of crystallization suggests that only 78% of the polymer crystallized. This indicates that some of the polymer was retained in the citronella-rich phase in a dissolved state.

### 3.2. Hot stage optical microscopy

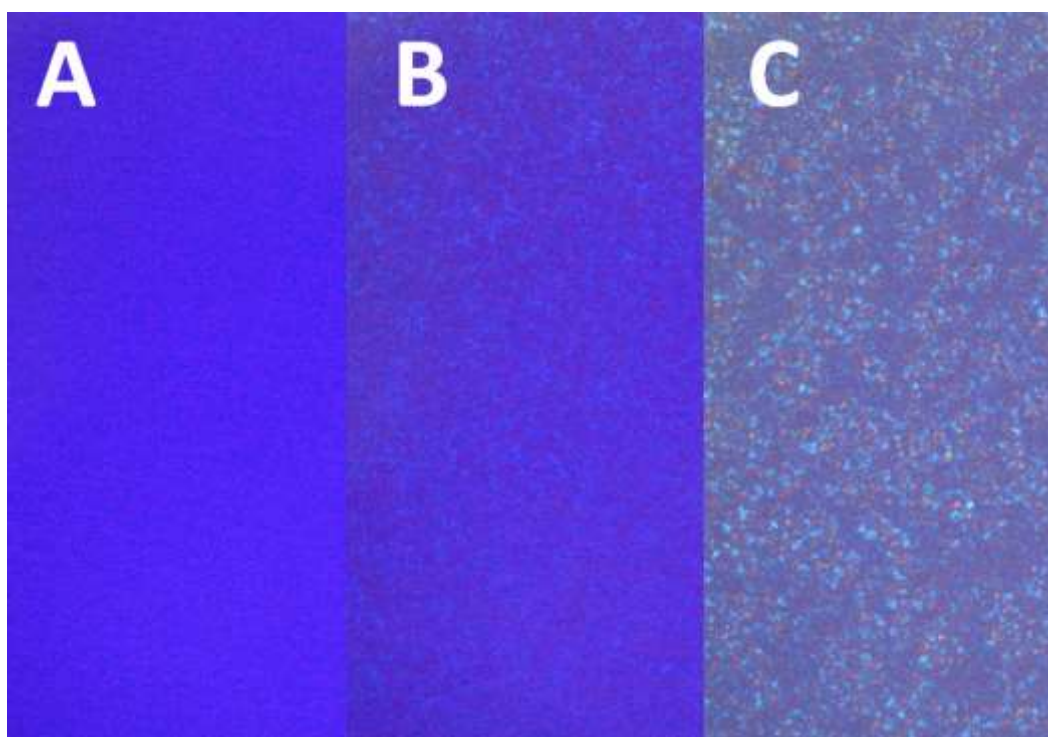


**Figure 3.** Optical micrographs of the phase changes in a binary system containing 30 wt.% LLDPE and 70 wt.% citronellal. (A) Homogeneous mixture at 140 °C; (B) Appearance of turbidity at 108 °C, and (C) the solidified crystalline material at 80 °C.

Figure 3 shows stages of phase change observed for a binary mixture with optical microscopy. Optical micrographs of LLDPE/Citronellal mixture were obtained using hot stage optical microscopy in order to determine the cloud point for each composition (appearance of turbidity). The samples were heated to a temperature well above the melting temperature of LLDPE where the two components were fully miscible. Subsequently, samples were cooled at a constant rate of  $10\text{ }^{\circ}\text{C min}^{-1}$ . At the cloud point a sudden appearance of numerous spots was observed. Finally, crystallization occurred in the mixture upon further cooling.

### 3.3 Phase diagram

The Flory-Huggins theory [9, 10] is one of the simplest theory describing the thermodynamics of polymer solutions. It is a lattice model in which it is assumed that each solvent molecule and polymer segment occupies exactly one lattice site. The Flory-Huggins model accounts for the effect of the great dissimilarity in the size of the polymer and solvent molecules on the entropy of mixing:

$$\Delta G_{mix} = RT[n_1 \ln \phi_1 + n_2 \ln \phi_2 + n_1 \phi_2 \chi] \quad (1)$$

where  $\Delta G_{mix}$  is the molar Gibbs free energy of mixing;  $n_1$  and  $n_2$  are the moles of solvent and polymer present respectively;  $\phi_1$  and  $\phi_2$  are the volume fractions of solvent and polymer respectively  $\chi$  is the Flory-Huggins interaction parameter;  $R$  is the gas constant and  $T$  is the absolute temperature. Equation (1) can be re-written as follows:

$$\Delta \bar{G}_{mix} = RT[(1 - \phi_2) \ln(1 - \phi_2) + (\phi_2/x) \ln \phi_2 + \chi(1 - \phi_2)\phi_2] \quad (2)$$

where  $\Delta \bar{G}_{mix}$  is the Gibbs free energy of mixing per mole of lattice sites and  $x$  is the ratio of the polymer molar volume to that of the solvent:

$$x = (M_{n,2}/\rho_2)/(M_1/\rho_1) \quad (3)$$

where  $M_{n,2}$  is the number average molecular weight of polymer,  $M_1$  is the molecular weight of the solvent and  $\rho_1$  and  $\rho_2$  are the densities of solvent and polymer respectively.

Upper critical solution temperature (UCST) phase behaviour is well accounted for by Flory-Huggins theory with the interaction parameter  $\chi$  exhibiting the following temperature dependence:

$$\chi = A + B/T \quad (4)$$

where  $A$  and  $B$  are constants and  $T$  is the absolute temperature.

The Flory-Huggins theory predicts the following for the critical point for the phase envelope:

$$\text{Critical composition: } \phi_{2,c} = 1/(1 + \sqrt{x}) \quad (5)$$



$$\text{Critical value of the interaction parameter: } \chi_c = 0.5 \left(1 + \sqrt{1/x}\right)^2 \quad (6)$$

The critical temperature can then be determined from equation (4).

McGuire *et al.* [11] presented two equations that relate the tie line compositions with the interaction parameter. They provide a simple method for extrapolating the co-existence or binodal curve (liquid–liquid phase boundary):

$$\left[ \left(\phi_2^\beta\right)^2 - \left(\phi_2^\alpha\right)^2 \right] \chi = \ln \left[ \left(1 - \phi_2^\alpha\right) / \left(1 - \phi_2^\beta\right) \right] + \left(1 - 1/x\right) \left(\phi_2^\alpha - \phi_2^\beta\right) \quad (7)$$

$$x \left[ \left(1 - \phi_2^\beta\right)^2 - \left(1 - \phi_2^\alpha\right)^2 \right] \chi = \ln \left( \phi_2^\alpha / \phi_2^\beta \right) + (x - 1) \left(\phi_2^\alpha - \phi_2^\beta\right) \quad (8)$$

where  $\phi_2^\alpha$  is the polymer's volume fraction in the polymer-poor phase and  $\phi_2^\beta$  is the polymer volume fraction in the polymer-rich phase.

The experimentally determined cloud points were assumed to be representative of the coexistence curve compositions. The interaction parameters  $\chi$  corresponding to each cloud point was calculated by simultaneously solving equations (7) and (8) based on the known  $\phi_2^\beta$  values. This yielded interaction parameter values as a function of temperature. These are plotted vs. the inverse of the absolute temperature, in Figure 4. The data conform to the linear relationship suggested by equation (4).

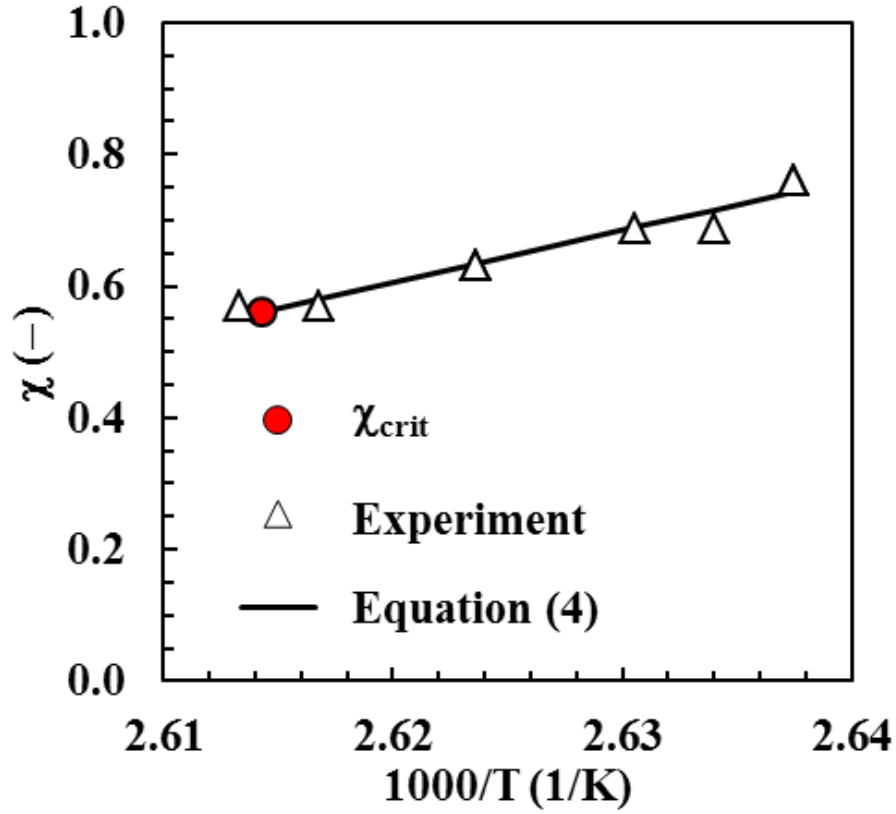


**Figure 4:** Temperature dependence of the Flory-Huggins interaction parameter for the system LLDPE-citronellal

Given the experimental determination of the interaction parameter, it is possible to predict the spinodal curve using the following expressions:

$$\phi_2^\beta = 1 - 1/\sqrt{2\chi} \quad (9)$$

$$1 + x\phi_2^\alpha/(1 - \phi_2^\alpha) - 2x\chi\phi_2^\alpha = 0 \quad (10)$$

Using all the above expressions, the binodal and spinodal coexistence curves were determined. They are plotted in Figure 5 along with the experimental cloud points. The generation of the coexistence curve in this manner is essentially an elegant curve fit based on the Flory-Huggins theory.

### 3.4. Melting point depression curve

Unfortunately it was not possible to experimentally verify the validity of the predicted spinodal curves at present. However, the applicability of the Flory-Huggins theory was checked by comparing the predicted melting point depression curve with experimental results. The former is done using the following expression [11],

$$T_m = \frac{1+(RB/\Delta H_u)(1-\phi_2)^2}{1/T_m^o+(R/\Delta H_u)[(1-1/x)(1-\phi_2)-(\ln \phi_2)/x-A(1-\phi_2)^2]} \quad (11)$$

where  $T_m$  is the melting of the diluted polymer,  $T_m^o$  is the melting point of the pure polymer and  $\Delta H_u$  is the heat of fusion per mole of the volume segments.

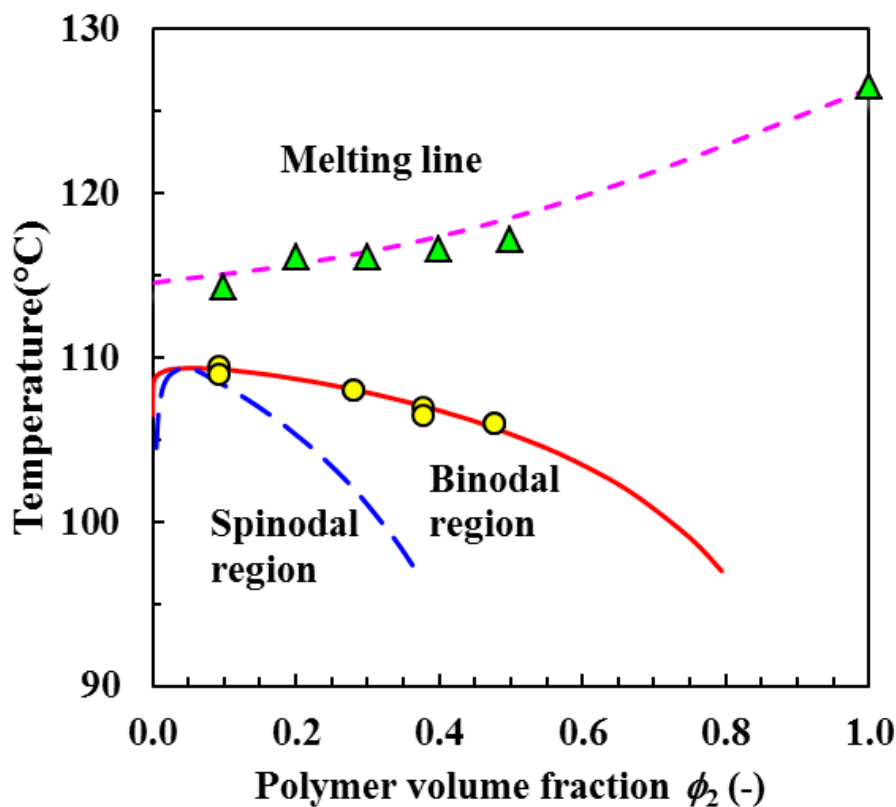


**Figure 5:** Experimental and predicted phase diagrams of LLDPE in Citronellal

The phase diagram of Figure 5 shows that, as expected, the binary LLDPE-citronellal system features UCST-type phase behaviour. Experimental DSC peak melting points of the mixtures

also coincided reasonably well with the predicted melt depression curve. Extrapolation of the binodal curve shows that at lower temperatures citronellal is very poorly soluble in LLDPE. The spinodal phase separation region is reached at a temperature of ca. 96.3 °C for an LLDPE concentration of 40 wt.%. However, since the phase separation is an exothermic event, the quench temperature should be set much lower in order to guarantee the formation of a microporous polymer.

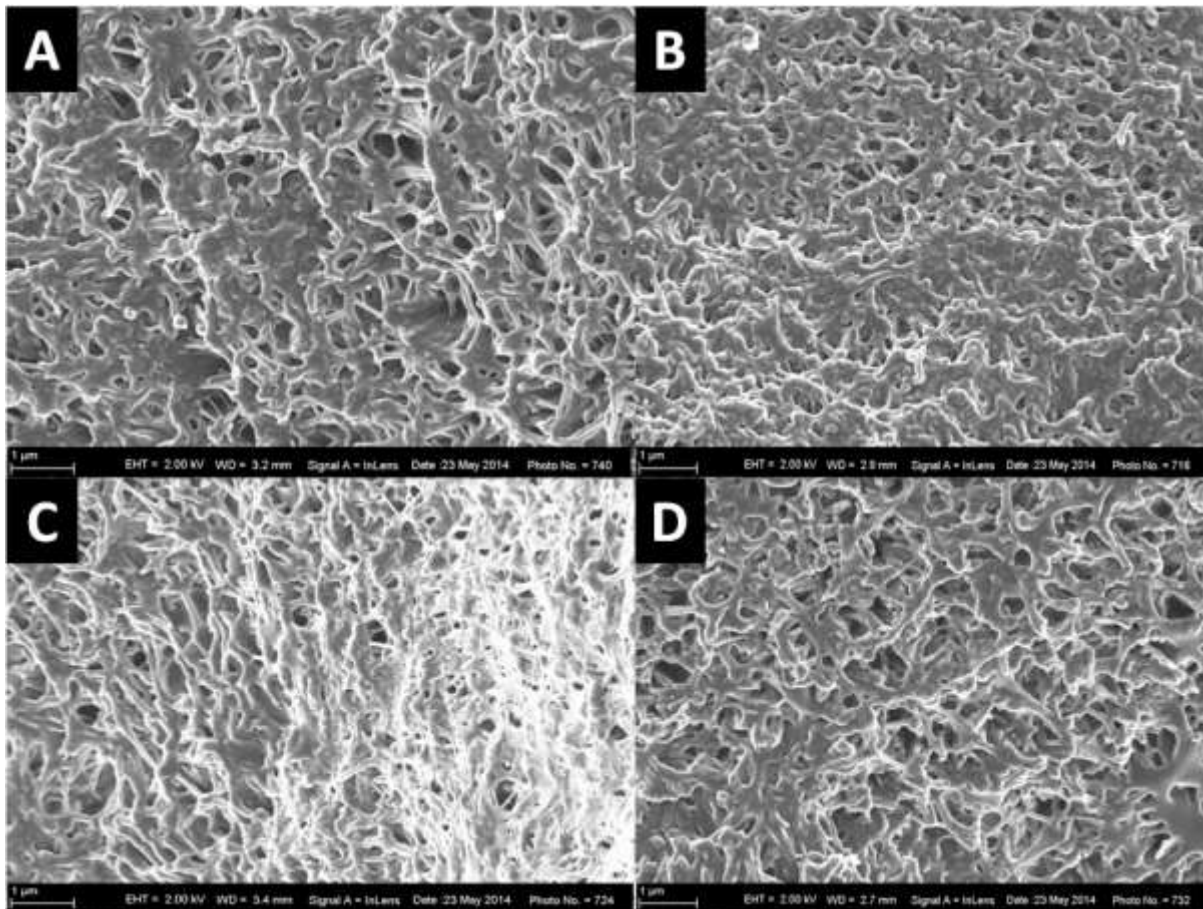


**Figure 6:** Scanning electron micrographs of TIPS microstructure for a LLDPE-citronellal 40:60 mass ratio blend prepared at different quenching temperatures. (A) -171 °C (liquid nitrogen); (B) -18 °C; (C) -14 °C, and (D) 5 °C.

### 3.5. Effect of the quenching temperature on morphology

Figure 6 shows the microporous morphologies obtained for a 40:60 LLDPE-citronellal blend at different quench temperatures. The quench temperatures varied from 5 °C to that of liquid

nitrogen. Over this temperature range all samples featured a similar morphology. The observed co-continuous structure suggests that the phase separation was indeed induced by spinodal decomposition. This behaviour was expected from the DSC results as well as the phase diagram obtained using Flory-Huggins thermodynamic model. Typical pore sizes in Figure 6 were less than 1  $\mu\text{m}$ . It is therefore likely that capillary forces effectively retain the liquid repellent in the fine open-cell polymer foam as they increase with decreasing pore diameter. Visual inspection indicated that the liquid-filled structure indeed behaved like a monolithic structure.

#### **4. Conclusions**

Binary mixtures of linear low density polyethylene and citronellal show upper critical solution temperature phase behaviour. The bimodal and the melting point depression curves were adequately fitted with Flory-Huggins theory. Quenching homogeneous melt mixtures resulted in a microporous structure with submicronic pores. This effectively solidified the liquid citronellal by trapping it inside the polymer framework and holding it by capillary forces.

#### **Acknowledgments**

The authors are grateful for financial support from Dr Leo Braack, the Centre for Sustainable Malaria Control at University of Pretoria and the National Research Foundation of South Africa.

#### **References**

- [1] A.J. Castro, Methods for making microporous products, in: US Pat 4247498, Axzona Inc, 1981.
- [2] D.R. Lloyd, K.E. Kinzer, H.S. Tseng, Microporous membrane formation via thermally induced phase separation. I. Solid-liquid phase separation, *Journal of Membrane Science*, 52 (1990) 239-261.
- [3] M. Ulbricht, Advanced functional polymer membranes, *Polymer*, 47 (2006) 2217-2262.

- [4] P. van de Witte, P.J. Dijkstra, J.W.A. van den Berg, J. Feijen, Phase separation processes in polymer solutions in relation to membrane formation, *Journal of Membrane Science*, 117 (1996) 1-31.
- [5] G.T. Caneba, D.S. Soong, Polymer membrane formation through the thermal-inversion process. 1. Experimental study of membrane structure formation, *Macromolecules*, 18 (1985) 2538-2545.
- [6] D.R. Lloyd, K.E. Kinzer, H.S. Tseng, Microporous membrane formation via thermally induced phase separation. I. Solid-liquid phase separation, *J. MEMBR. SCI.*, 52 (1990) 239-261.
- [7] D.R. Lloyd, S.S. Kim, K.E. Kinzer, Microporous membrane formation via thermally-induced phase separation. II. Liquid-liquid phase separation, *Journal of Membrane Science*, 64 (1991) 1-11.
- [8] D.W. Lee, C.M. Jensen, Dry-Ice Bath Based on Ethylene Glycol Mixtures, *J Chem Educ*, 77 (2000) 629.
- [9] P.J. Flory, Thermodynamics of high polymer solutions, *The Journal of Chemical Physics*, 9 (1941) 660-661.
- [10] M.L. Huggins, Solutions of long chain compounds, *The Journal of Chemical Physics*, 9 (1941) 440.
- [11] K.S. McGuire, A. Laxminarayan, D.R. Lloyd, A simple method of extrapolating the coexistence curve and predicting the melting point depression curve from cloud point data for polymer-diluent systems, *Polymer*, 35 (1994) 4404-4407.